RESEARCH ARTICLE

Effects of the North Atlantic Subtropical High on summertime precipitation organization in the southeast United States

Rosana Nieto Ferreira [ORCID] | Thomas M. Rickenbach

Department of Geography, Planning and Environment, East Carolina University, Greenville, North Carolina

Correspondence
Rosana Nieto Ferreira, Department of Geography, Planning, and Environment, A-227 Brewster Bldg., East Carolina University, Greenville, NC 27858-4353.
Email: ferreirar@ecu.edu

Abstract

This study analyzes the effect of the location of the North Atlantic Subtropical High (NASH) western ridge on the daily variability of precipitation organization in the southeastern United States (SE US). The western side of the NASH, also known as the NASH western ridge, plays an important role in the variability of summertime precipitation in this region. In this study, the mean summertime position of the NASH western ridge was determined and used to classify each summer day during 2009–2012 into one of four quadrants. Composites of synoptic-scale circulation and precipitation from mesoscale and isolated precipitation features (MPF and IPF) were calculated for each NASH western ridge quadrant. MPF contributed most (about 65%) of the total summertime precipitation and accounted for most of the differences between the four NASH quadrants. Domain-averaged precipitation was highest (lowest) during NASH-SW (NASH-NW) when IPF (MPF) precipitation was strongest (weakest). The regionality of MPF precipitation maxima was generally associated with the location of low-level jets and upper-level troughs. For instance, positive MPF anomalies occurred across the SE US during NASH-SW when the Great Plains low-level jet turned eastward bringing moisture to fuel convection in the SE US. In contrast, IPF rain was distributed more uniformly across the SE US. Finally, this study revealed a dipole of precipitation that is controlled by the position of the NASH western ridge and its associated low-level jets. In one extreme of the dipole NASH-SE, periods are associated with enhanced MPF precipitation along the coast and offshore for days at a time, and suppressed MPF precipitation inland. The opposite pattern occurs during NASH-NW when MPF precipitation is enhanced inland and suppressed along the coast and offshore.

KEYWORDS
North Atlantic Subtropical High, precipitation dipole, summertime precipitation organization

1 | INTRODUCTION

The North Atlantic Subtropical High (NASH) is a dominant climatological feature that has significant impacts on both sides of the Atlantic (e.g., Davis *et al.*, 1997; Cherchi *et al.*, 2018). During summer when midlatitude cyclone tracks shift northward of 45°–50°N, the NASH is manifested as a strong pressure maximum located in the

central Atlantic and extending from North America to Europe (e.g., Davis et al., 1997). In the Americas the western side of the NASH, known as the NASH western ridge, controls seasonal moisture transport, vertical motion, and precipitation in the southeastern United States (SE US) and the Caribbean (Li et al., 2011; Bishop et al., 2019). Likewise, on the other side of the Atlantic the Iberian Peninsula (Spain and Portugal) experiences changes in precipitation depending on the location of the eastern ridge of the NASH (Cortesi et al., 2014, compare their figs. 7 and 8).

The effect of the NASH on SE US precipitation variability is realized via the location of the NASH western ridge and its control on low-level flow, sea level pressure, and vertical motion. In particular, the NASH western ridge controls the location and intensity of the three low-level jets (LLJs) that play an important role in helping modulate the moisture budgets and precipitation in the central and eastern United States, namely the southerly Great Plains LLJ (GPLLJ; e.g., Higgins et al., 1997; Doubler et al., 2015; Wei et al., 2019), the Caribbean low-level jet (e.g., Muñoz et al., 2008), and a third jet feature over the Gulf Stream in the western Atlantic (Zhang et al., 2006; Colle and Novak, 2010; Helmis et al., 2013). More recently, the NASH has been shown to affect the northern branch of the South American low-level jet and precipitation in South America (Jones, 2019). The location and strength of the NASH and the GPLLJ have also been shown to affect surface ozone concentrations and air quality in coastal urban regions along the Gulf of Mexico (Wang et al., 2016), the trajectory of tropical cyclones (Colbert and Soden, 2012), and the timing of the North and South American monsoons (Arias et al., 2012).

Previous studies have shown that the NASH affects precipitation in the SE US on timescales that range from diurnal to multi-decadal (e.g., Diem, 2006; Li et al., 2011, 2012, 2013; Bishop et al., 2019; Schmidt and Grise, 2019). On daily timescales, Luchetti et al. (2017) found that the NASH western ridge helps control moisture availability and winds along the North Carolina coast, thus providing a synoptic-scale control mechanism for sea breeze precipitation. In particular, they showed that when the NASH western ridge is located along the southeast coast of the United States, its associated moist southwesterly flow along the North Carolina coast favours the occurrence of precipitation along the sea breeze front.

On intraseasonal timescales, wet periods in the SE US have been found to be associated with the presence of a mid-to-upper tropospheric trough combined with the presence of the western side of the NASH (Diem, 2006). Dry periods on the other hand were found to be associated with generally anticyclonic circulation and weak

lower tropospheric flow over the SE US, along with a mid-tropospheric trough that is located further eastward over the Atlantic (Diem, 2006). More recently Wei et al. (2019) described a mode of intraseasonal variability of SE US summertime precipitation on timescales of 10–20 days that they hypothesize is maintained by interactions with the NASH and the GPLLJ.

On seasonal timescales, Li et al. (2012) classified the summertime NASH into four categories or quadrants according to the location of the westernmost point of the NASH western ridge with respect to its climatological mean position in the Gulf of Mexico, just offshore from the Florida Panhandle. They found that changes in the position of the NASH western ridge cause significant interannual precipitation variability in the SE US, with increased moisture transport and precipitation during summers when the NASH western ridge is located to the southwest of its mean position. The opposite occurs when the NASH western ridge is located northwest of the mean position. On multi-decadal timescales the NASH western ridge has been shown to have shifted westward between 1948 and 1977 (Li et al., 2011) and eastward from 1978–2007 (Diem, 2013a; 2013b). Some of this variability has been linked to the influence of stationary wave trains driven by the Pacific Decadal Oscillation (Li et al., 2011; 2013) as well as to a possible intensification and expansion of the NASH during this period (Li et al., 2011; He et al., 2017; Schmidt and Grise, 2019).

Although the seasonal mean variability of the NASH western ridge and its effect on precipitation totals in the SE US has been previously studied, the daily variability of the NASH western ridge and its effect on the daily precipitation organization in the SE US have not been explored. Rickenbach et al., 2015, hereafter R15) used a high-resolution radar-based precipitation dataset to study the organization of precipitation in the SE US. They classified precipitation features based on their size either as isolated precipitation features (IPF) that are smaller than 100 km or as larger, mesoscale precipitation features (MPF). Previous studies established that MPF are generally associated with synoptic-scale dynamical forcing including easterly waves in the Tropics (Leary and Houze, 1979), synoptic ascent in frontal regions of mid-latitude cyclones, or the divergent region of jet stream troughs (Houze et al., 1990; Laing and Fritsch, 2000; Parker and Johnson, 2000; R15), whereas IPF tend to form in response to local-scale thermal circulations (Wallace, 1975; R15). In particular, R15 found that this size-based precipitation organization framework revealed significant differences in the diurnal and seasonal variability of IPF and MPF that were indicative of their different forcing mechanisms. For instance, they found that the more thermally forced IPF have a strong diurnal and

seasonal cycle, whereas the more dynamically forced MPF do not. Rickenbach (2018) used the R15 dataset to study extreme precipitation associated with IPF and MPF in the SE US and found that about 60% of all extreme summertime precipitation pixels were associated with MPF. More recently, Rickenbach et al. (2020) used the R15 dataset to show that the springtime transition to the summer IPF in the SE US shares some similarities with the onset of the monsoon.

The goals of this study are to (a) investigate the daily variability of the position of the NASH western ridge; (b) study how the position of the NASH western ridge affects the organization of precipitation in the SE US; (c) analyse the synoptic scale characteristics of the NASH western ridge that may control precipitation organization in the SE US such as the position and strength of the moisture-laden low-level jets on the western side of the NASH; and (d) identify regional patterns of precipitation organization associated with the NASH. Section 2 presents the datasets and methodology, Section 3 presents results, and the discussion and conclusions are presented in Sections 4 and 5.

2 | DATASETS AND METHODOLOGY

This study uses the R15 daily precipitation organization dataset available from 2009 to 2012, daily precipitation from the high-resolution National Aeronautics and Space Administration (NASA) Tropical Rainfall Measurements Mission (TRMM; Huffman et al., 2007), dynamic and thermodynamic fields from the daily North American Regional Reanalysis (NARR; Mesinger et al., 2006) at 32 km horizontal resolution, and the National Center for Environmental Prediction and National Center for Atmospheric Research Reanalysis (NCEP–NCAR; Kalnay et al., 1996), at 2.5° horizontal resolution.

2.1 | Determination of the position of the NASH western ridge

Various methodologies have been used previously to determine the location of the NASH western ridge. Li et al. (2011) and Diem (2013a) defined the westernmost point of the NASH western ridge as the location where the seasonal-mean 850 hPa surface's 1,560 m geopotential contour crosses the NASH ridge line, defined as the line where the zonal wind (u) equals zero, and $\frac{\partial u}{\partial y} > 0$. In the West Atlantic, the NASH ridge is defined as the line where $u = 0$ (where the u wind changes direction) and $\frac{\partial u}{\partial y} > 0$ so that easterlies on the equatorward side of the

NASH reverse to westerlies on the poleward side of the NASH. Since the seasonal mean summertime NASH has a nearly elliptic shape across the Atlantic, on seasonal timescales this method yields a single point along the western side of the 1,560 m geopotential contour where $u = 0$ and $\frac{\partial u}{\partial y} > 0$. Those studies used the 850 hPa geopotential level to avoid complications associated with terrain (such as the Appalachian Mountains), and the 1,560 m contour because it tends to follow the maxima in summertime precipitation and upward motion along the western flank of the NASH (see fig. 1 of Li et al., 2012). Other studies simply used the 1,560 m geopotential contour to follow north–south displacements of the NASH western ridge (Bowerman et al., 2017) or monthly varying reference geopotential contours (Wang et al., 2016). The discussion above highlights that there is a degree of subjectivity in the choice of a reference geopotential contour to study the NASH western ridge.

The method used here for determining the daily location of the western edge of the NASH western ridge largely follows Li et al. (2012) and Diem (2013a), except for using daily rather than seasonal averages and a more simplified method for determining the location of the westernmost point of the NASH western ridge (as in Wei et al., 2019). The use of a constant reference contour to determine the NASH western ridge location is arbitrary but intentional since it allows the study of the monthly progression of the frequency of the NASH location in each quadrant. Also, the 1,560 m geopotential contour at 850 hPa allows the results herein to be more directly compared to the seasonal averages presented in Li et al. (2012) and Diem (2013a). The method used here consists of three steps: (a) find the outline of the 1,560 m geopotential height contour at 850 hPa, (b) check that it extends eastward of 70°W to confirm that the contour is part of the NASH, and (c) identify the westernmost point of the contour which will be simply referred to as the NASH western ridge.

The need to relax the Li et al. (2011) criteria to determine the daily position of the NASH western ridge arises because the daily 1,560 m geopotential contour often has a more irregular shape than the seasonal averaged 1,560 contour. In the daily plots, there can be more than one point along the 1,560 m geopotential contour where the Li et al. (2011) criteria are obeyed and therefore more than one NASH western ridge location could be defined. In contrast, the definition of the NASH western ridge as the westernmost point along the 1,560 m contour yields a single point. A comparison of the daily NASH western ridge positions obtained using our methodology and the Li et al. (2011) methodology for June–August 2009–2012 showed that on most days the intersection of the $u = 0$ contour and the 1,560 m geopotential contour fell on or

very close to the westernmost point of the 1,560 m geopotential contour. Thus, on average the location of the western ridge calculated using our method was 0.6° to the south and 0.2° to the west of the western ridge calculated using the Li *et al*. (2011) method. This suggests that the westernmost point of the 1,560 m geopotential contour is a reasonable choice for detecting the westernmost location of the NASH western ridge. In fact, Wei *et al*. (2019) make this same choice in their recent study of intraseasonal variability of precipitation in the SE US.

Determination of the daily location of the NASH western ridge was not straightforward when the 1,560 m contour was split into two or when the NASH did not extend across the Atlantic. On days when the 1,560 m contour was split into two the contour that was connected to the main body of the NASH over the Atlantic was subjectively chosen. Days when the 1,560 m contour did not extend across the Atlantic (June 1–6, 2011) were excluded from this study. Also excluded from this study were days when the NASH western ridge was present outside the eastern border of NARR domain (a total of 15 days). In total, 21 days during June–August 2009–2012 were excluded from this analysis.

2.2 | NASH western ridge classification

To analyse the effect of the NASH western ridge on the synoptic-scale flow and precipitation organization in the SE US, the position of the NASH western ridge was classified into four categories based on its mean 2009–2012 summertime position. The domain was divided into four quadrants and each day was labelled as either northwest (hereafter NASH-NW), southwest (NASH-SW), northeast (NASH-NE), or southeast (NASH-SE), depending on the quadrant where the NASH western ridge was located on that day. Based on the daily NASH western ridge classification, composites of NARR geopotential, winds, and moisture fluxes were calculated. The 850 hPa moisture flux, defined as $(u + v) \cdot q$, where u and v are the zonal and meridional winds and q is the specific humidity, was used to indicate the availability of moisture to fuel convection. Composites of environmental convective available potential energy (CAPE) and convective inhibition (CIN) from NARR were also examined.

2.3 | Precipitation from TRMM

The relationship between the NASH and precipitation variability over the Atlantic and SE US was also analysed using composites of the TRMM-3B42 daily precipitation dataset. TRMM combines passive microwave and radar measurements with geosynchronous satellite cloud-top

data to produce homogeneous spatial and temporal precipitation coverage, adjusted with rain gauges over land, from 50°N to 50°S at 0.25° resolution (Huffman *et al*., 2007). Fig. 6 in R15 shows that there is good agreement between the 2009 and 2012 average precipitation from the National Mosaic and Multi-sensor Quantitative Precipitation Estimation (NMQ-Q2) radar product (Zhang *et al*., 2011) and the TRMM satellite 3B-42 product over the SE US.

2.4 | Precipitation organization

This study uses daily R15 IPF and MPF precipitation to create composites of total, IPF and MPF precipitation for each NASH western ridge regime. The R15 precipitation organization dataset is available from 2009 to 2012 at 15-min, 1-km grid spacing over the domain shown in Figure 1. R15 used the National Mosaic and Multi-sensor Quantitative Precipitation Estimation (NMQ – "Q2"; Zhang *et al*., 2011) radar-based precipitation dataset, a state-of-the-art estimation of precipitation rate constructed from the national Doppler radar network, to classify precipitation into IPF and MPF as follows. For each 15-min snapshot of the NMQ precipitation, R15 identified all contiguous precipitation features that met a threshold of 0.5 mm·hr^{-1} in the SE US and objectively classified them according to their size into either IPF smaller than 100 km or larger MPF. The NMQ is well suited for this study because its high temporal frequency, horizontal resolution and homogeneity over the SE US make it possible to capture even small, short-lived IPFs. For further details on the precipitation feature organization algorithm, the reader is referred to R15. The "NMQ domain" is hereafter defined as the region where the NMQ data is available in R15, that is, the land and light grey ocean areas shown in Figure 1. Daily total, IPF and MPF precipitation, and daily domain averages were determined from the NMQ data.

3 | RESULTS

During the summer, the NASH western ridge position migrated between the four quadrants on daily-to-seasonal timescales. The effects of this migration on regional winds and precipitation amounts and organization in the eastern United States are studied below.

3.1 | Variability of the daily position of the NASH western ridge

To compare our methodology and datasets to previous studies, the seasonal mean average position of the NASH

FIGURE 1 "NMQ domain" over land (grey) and ocean (light grey). Note that there is no NMQ data over the dark grey ocean region
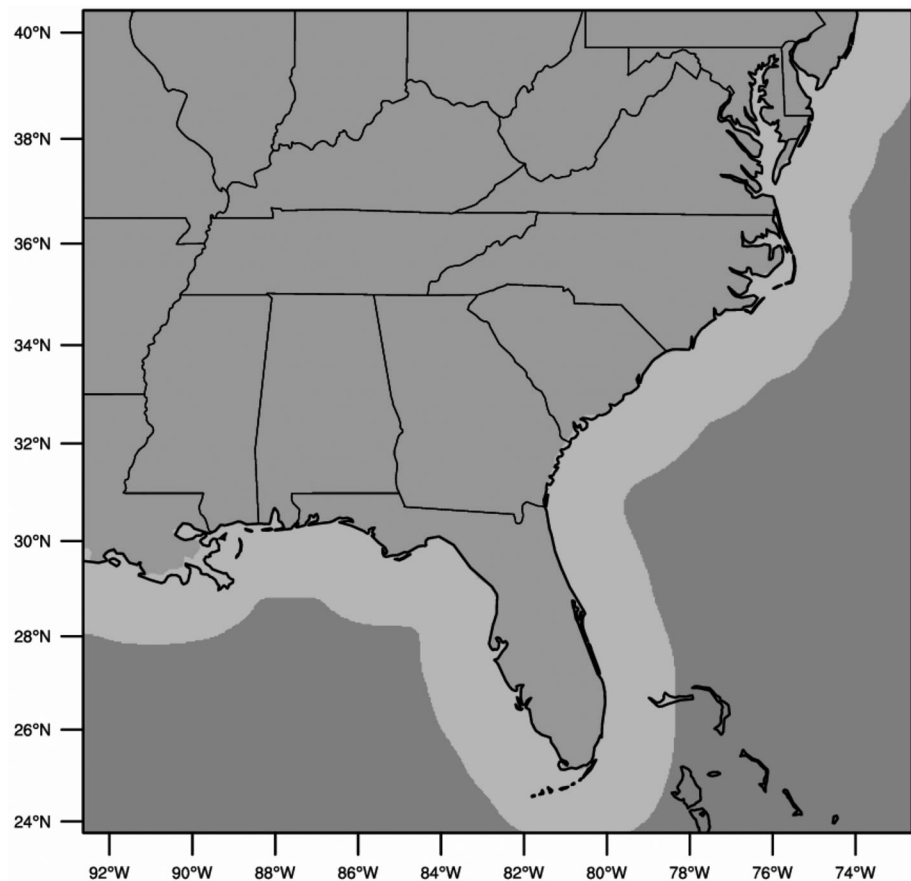

western ridge was estimated using NARR and the NCEP Reanalysis. During JJA 2009–2012 the average position of the NASH western ridge was 86°W, 28°N (crosshair position in each panel of Figure 2) in NARR and 84°W, 29°N in the NCEP Reanalysis. This is a distance of about 225 km (one gridpoint) which indicates good agreement between the two datasets and good agreement also with the 1948–2007 mean summertime position of the NASH western ridge in Li *et al.* (2011) which was 86°W, 27°N. As mentioned in the previous section, the analysis presented below uses the higher resolution NARR dataset. Hence, the study domain was divided into four quadrants centred on the climatological position of the NASH western ridge in NARR at 86°W, 28°N (Figure 2).

The position of the NASH western ridge changed on day-to-day and month-to-month timescales. During JJA 2009–2012, the NASH western ridge was located in the NASH-NW (139 days) and NASH-SE (119 days) quadrants 74% of the time (Table 1). The remainder of the time the NASH western ridge was in the NASH-NE (34 days) and NASH-SW (55 days) quadrants. Figure 2 shows the daily positions of the NASH western ridge during June–August 2009–2012. The location of the NASH western ridge had a clear monthly progression. In June, it was located about 65% of the time in the eastern quadrants, and mostly in the SE quadrant (Table 1). In July,

the NASH western ridge shifted westward spending about 80% of the days in the western quadrant, and mostly in the NW quadrant (Table 1). In August, the NASH spent most of the days (75%) in the SE and NW quadrants (Table 1).

Superimposed on the monthly pattern of a westward shift in early summer followed by an eastward retreat in late summer (Figure 2), there was also a distinct intraseasonal variability of the NASH western ridge position (Figure 3) characterized generally by clustering in time between the SE and NW quadrants. Over the four summers only 11% of the NASH-NW days were single-day events while about 75% of days were part of a sequence of consecutive days that lasted from 4 days to nearly 2 weeks. The longest NASH-NW sequence lasted 12 days in July of 2012. The NASH-SE displays similar clustering with about 13% single-day events and 67% of the sequences lasting 4 days or longer. A very long-lasting NASH-SE sequence occurred in June 2009. One exception was 2011 when the NASH western ridge alternated between the NASH-SE and NASH-NW every few days, rather than spending longer time periods in the same quadrant (Figure 3). On the other hand, all of the NASH-SW and NASH-NE sequences lasted less than 4 days, indicating that the NASH western ridge remained in the SW and NE quadrants for short periods of time.
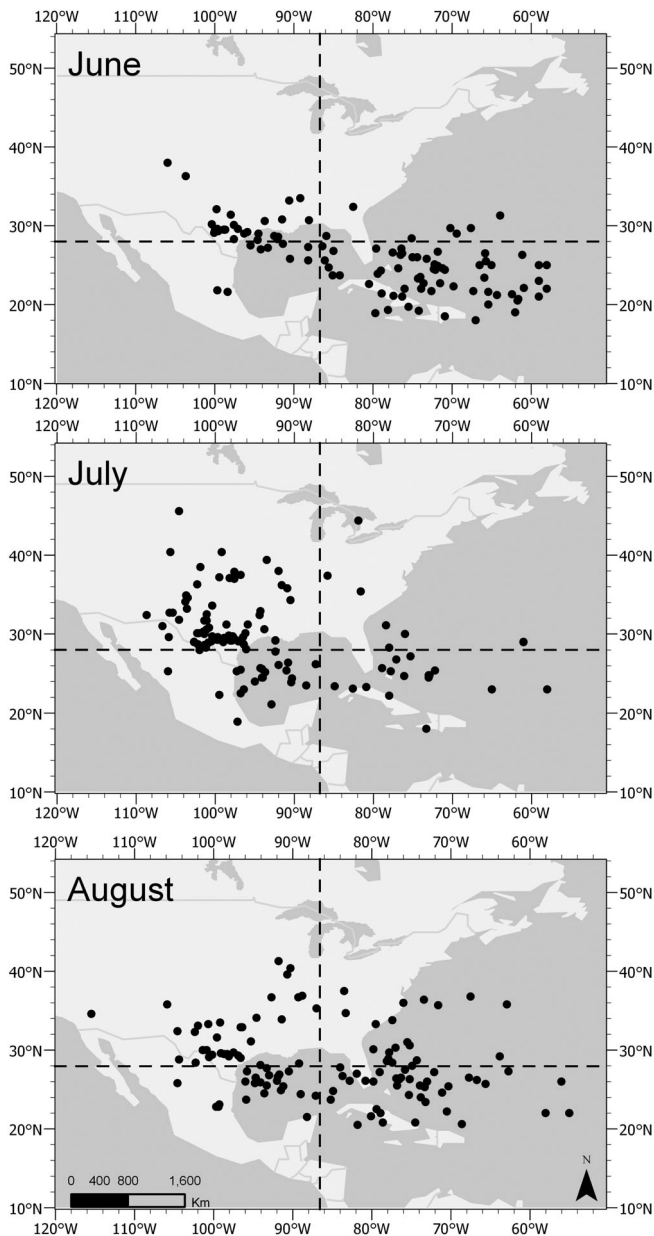
FIGURE 2 Daily NASH western ridge position (black circles) for June (top panel), July (middle panel), and August (bottom panel) 2009–2012. Dashed lines delineate the four quadrants used to classify the NASH western ridge

3.2 | NASH western ridge and variability of atmospheric circulation and total precipitation

This section examines the relationship between the position of the NASH western ridge and the winds and precipitation in the SE US, focusing on the 4 years (2009–2012) for which the R15 precipitation organization data is available.

The role of the NASH western ridge in helping establish the location of low-level jets and precipitation in and around the SE US is analysed using the composites in

TABLE 1 Total number of days that the NASH western ridge was located in each quadrant per month, as well as monthly and quadrant totals

	NW	SW	NE	SE	Total
June	27	10	7	63	107
July	76	22	7	17	122
August	36	23	20	39	118
Total	139	55	34	119	347

Figures 4 and 5. Figure 4 shows the composite TRMM precipitation, 850 hPa NARR winds and 850 hPa geopotential for each NASH western ridge quadrant. Figure 5 shows the 850 hPa moisture flux along with the geopotential height for each NASH western ridge quadrant. The 1,560 m geopotential contour is highlighted in each figure to aid the visualization of the differences in NASH western ridge position. Strong southwesterly winds and maxima in precipitation generally occurred westward of the 1,560 m geopotential contour in each composite (Figure 4). The three LLJs (GPLLJ, Caribbean LLJ, and Western Atlantic LLJ) along the western side of the NASH acted as rivers of moisture (Figure 5) that fuelled precipitation in different parts of the United States, Atlantic Ocean, and Caribbean as the NASH western ridge shifted position (Figure 4). Those three rivers of moisture were present in all four composites.

The role of the GPLLJ on funnelling moisture to fuel precipitation in the SE US was more prominent when the NASH western ridge was located in the western quadrants (NASH-NW and NASH-SW, Figure 4a,c) than in the eastern quadrants (NASH-NE and NASH-SE, Figure 4b,d). During NASH-NW and NASH-SW (Figure 5a,b) the GPLLJ (between 90°W and 100°W) and its associated moisture fluxes were about 40% stronger compared to NASH-NE and NASH-SE (Figure 5b,d). In particular, the NASH-NW composite had a strong GPLLJ that extended northward to the Canadian border and then eastward across the Great Lakes. This means that on NASH-NW days the GPLLJ bypassed the southern tier of the SE US and adjoining ocean areas, leaving these areas generally drier (Figure 4a) when compared the other composites (Figure 4b–d). Combined with the fact that NASH-NW periods often lasted 5 days and longer (see Figure 3), this means that portions of the SE US can experience prolonged dry spells during NASH-NW events. On the other hand, the GPLLJ in the NASH-SW composite turned eastward at a lower latitude (Figure 4c) thus bringing moisture to fuel precipitation in the SE US. The NASH-SW composite in fact has the strongest moisture fluxes into the SE US (Figure 5) and more widespread precipitation across the SE US (Figure 4) than the other composites.
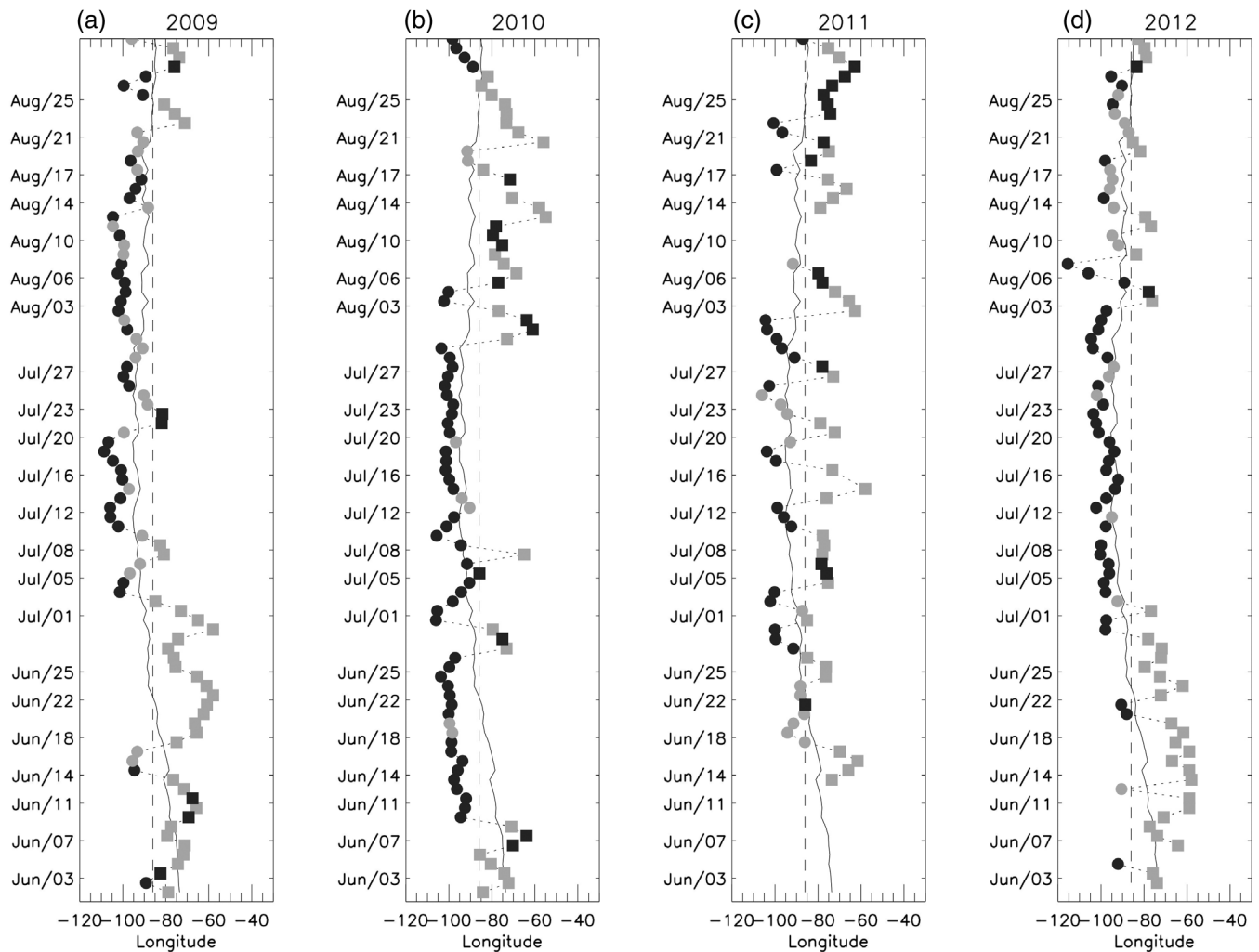
FIGURE 3 Time series of the daily summertime position of the NASH western ridge for 2009–2012, with NASH-NW represented by black circles, NASH-SW by grey circles, NASH-NE by black squares, and NASH-SE by grey squares. The solid grey line shows the time series of the climatological mean daily position of the NASH western ridge in the NCEP Reanalysis for 1948–2018. The dashed grey line shows the mean JJA position of the NASH western ridge in the NCEP Reanalysis for 1948–2018

In turn, when the NASH western ridge was located in one of the eastern quadrants (NASH-NE and NASH-SE) the NASH circulation appeared to become disconnected from the GPLLJ (Figure 4b,d) and its associated moisture fluxes (Figure 5b,d). During NASH-NE, the strongest precipitation was concentrated along the western Atlantic low-level jet that flowed northward along the western side of the NASH offshore from the East Coast of the United States (Figure 4b). Finally, during NASH-SE the region of strongest precipitation stretched northeastward from the eastern Gulf of Mexico, through Florida and into the North Atlantic, along the western side of the NASH and following the western Atlantic low-level jet (Figure 4d).

At 500 hPa, the northern (NASH-NW and NASH-NE) composites were characterized by a more zonal flow and a jet stream that was stronger and located farther north

(Figure 6a,b). The southern (NASH-SW and NASH-SE) composites on the other hand had a weaker jet stream and a more meridional flow in the mid-troposphere (Figure 6c,d). In particular, the NASH-SW composite (Figure 6c) had a 500 hPa trough that dug southward into the SE US providing synoptic-scale forcing for organized precipitation, in agreement with Diem (2006). The NASH-SE composite (Figure 6d) had a 500 hPa trough that was located further east, along the coast, providing synoptic-scale forcing for organized precipitation over Florida and just offshore of the U.S. eastern seaboard.

These changes in tropospheric circulation, and in particular the changes in the position and strength of the upper-level jet stream and low-level jets associated with the NASH western ridge likely affect precipitation organization in the SE US. The next subsection investigates this hypothesis.
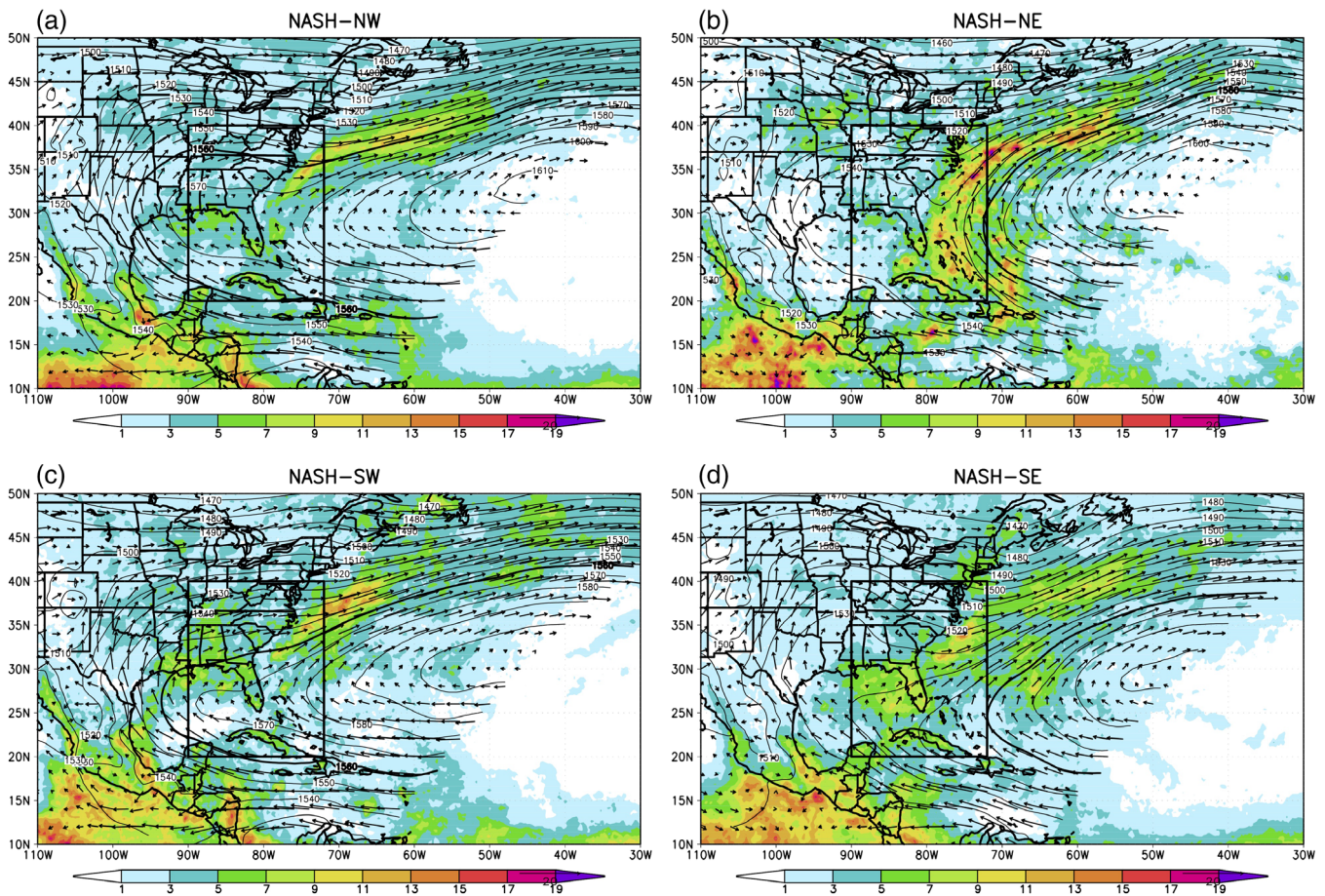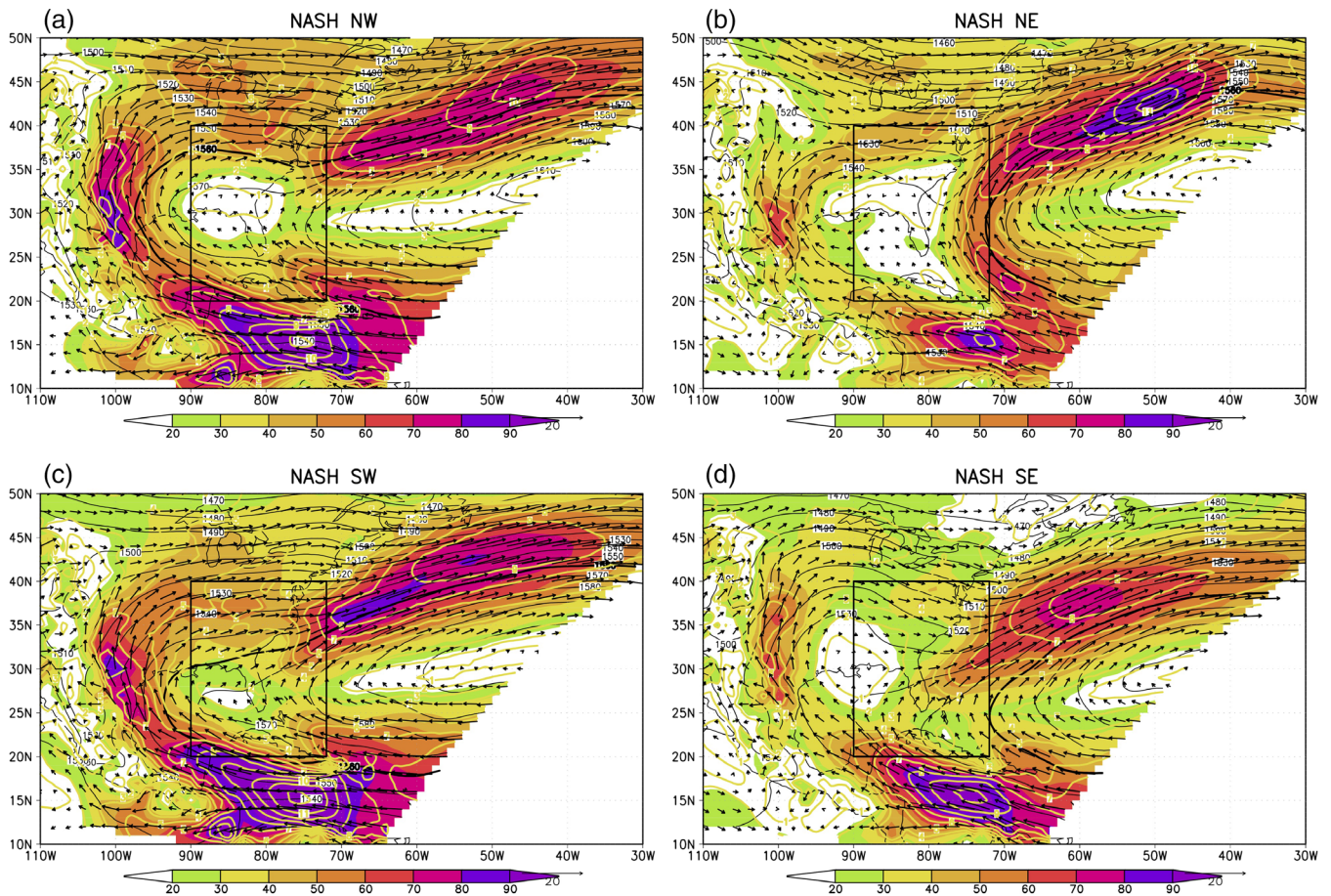
FIGURE 4 Composites of TRMM precipitation (shaded, mm·day^{-1}), and NARR 850 hPa winds (vectors, m·s^{-1}), and geopotential height (contours, m) for each NASH western ridge regime. The 1,560 m contour is thicker and boxes mark the location of the NMQ domain [Colour figure can be viewed at wileyonlinelibrary.com]

3.3 | NASH western ridge and precipitation organization

A first look at how the position of the NASH western ridge affects precipitation organization is presented in Table 2, which shows the R15 NMQ domain area averaged total, IPF and MPF precipitation for each NASH western ridge composite. As shown in the previous subsection, the location of the NASH western ridge affects the synoptic scale circulation in a broad area that encompasses the NMQ domain. This means that the location of the NASH western ridge does not have to fall within the NMQ domain to affect precipitation within the NMQ domain. The total domain-averaged summertime precipitation during 2009–2012 was 3.49 mm·day^{-1} with 65% of the total in the MPF category. This MPF rain fraction, within a few percent of this value for each quadrant, was generally consistent with the summertime climatology of mesoscale rain fraction in the SE US presented in R15 and Nesbitt *et al.* (2006). The anomalies from the all-days averages are also shown in Table 2. Comparison of the

domain-averaged precipitation for each NASH quadrant to the overall summertime average shows that NASH-NW was the driest composite with domain-averaged precipitation that was about 8% drier than the summertime average, and nearly all of the deficit due to a 0.27 mm·day^{-1} decrease in MPF precipitation when compared to the summertime mean. In contrast NASH-SW was the rainiest composite with total domain-averaged precipitation that was 0.28 mm·day^{-1} (8%) higher than average, a surplus that was contributed by increases in MPF (0.19 mm·day^{-1}), and to a lesser extend in IPF (0.09 mm·day^{-1}). In terms of IPF, NASH-SW had the largest IPF precipitation amount of all composites (1.31 mm·day^{-1} or 7% above the all-day IPF average) while NASH-SE had the lowest values of IPF precipitation (1.16 mm·day^{-1} or 5% lower than the all-day IPF average). NASH-NW and NASH-NE had similar domain-averaged IPF precipitation.

Although the differences in domain-averaged precipitation between the NASH-SW (3.77 mm·day^{-1}), NASH-NE (3.70 mm·day^{-1}), and NASH-SE (3.63 mm·day^{-1})

FIGURE 5 Composites of NARR 850 hPa moisture fluxes (shaded, $g \cdot kg^{-1} \cdot m \cdot s^{-1}$), geopotential height (contours, m), and winds (vectors, $m \cdot s^{-1}$) for each NASH western ridge regime. The 1,560 m contour is thicker and boxes mark the location of the NMQ domain [Colour figure can be viewed at wileyonlinelibrary.com]

composites were relatively modest, notable differences occurred in their regional patterns of precipitation. The regional patterns of total, IPF, and MPF precipitation anomalies for each composite are shown in Figure 7.

Recall that the two rainiest composites, NASH-SW and NASH-NE, were characterized by positive domain-averaged IPF and MPF precipitation anomalies (Table 2). Figure 7 shows that while the positive IPF precipitation anomalies in NASH-SW (Figure 7e) and NASH-NE (Figure 7h) were evenly distributed throughout the domain, the positive MPF anomalies in NASH-SW (Figure 7f) and NASH-NE (Figure 7i) had distinct regionality that was likely linked to the synoptic-scale circulation patterns. The NASH-SW composite had 850 hPa westerly and southwesterly winds across the SE US (Figure 4c), associated with an eastward-turning GPLLJ that brought moisture into the region (Figure 5c). The strongest positive MPF precipitation anomalies in NASH-SW were located on the windward side of the Appalachian Mountains, with weaker MPF precipitation anomalies on the lee side of the Appalachian Mountains, suggestive of the presence of an orographic effect (R15;

Parker and Ahijevych, 2007). In NASH-NE, positive MPF precipitation anomalies (Figure 7i) occurred to the east of the Appalachian Mountains in the mid-Atlantic coastal plain, a region where low-level moisture fluxes associated with the western Atlantic low-level jet converged with midlatitude westerly winds (Figure 5b).

The NASH-SE composite (Figure 7j) had positive precipitation anomalies along the Gulf Coast, across Florida, and offshore over the western Atlantic. These positive anomalies were due mostly to enhanced MPF precipitation (Figure 7l) which was likely associated with the presence of an eastward-shifted 500 hPa trough (Figure 6d) and a strong Western Atlantic LLJ that guided moisture across Florida and the Western Atlantic (Figure 5d). Inland, the NASH-SE composite had negative MPF (Figure 7l) and IPF (Figure 7k) precipitation anomalies. Finally, the driest composite, NASH-NW, was characterized by a NASH western ridge that extended westward beyond the NMQ domain producing anomalous high 850 hPa geopotential and anticyclonic winds (Figure 4a) in the NMQ domain that tended to suppress precipitation leading to overall negative MPF precipitation anomalies
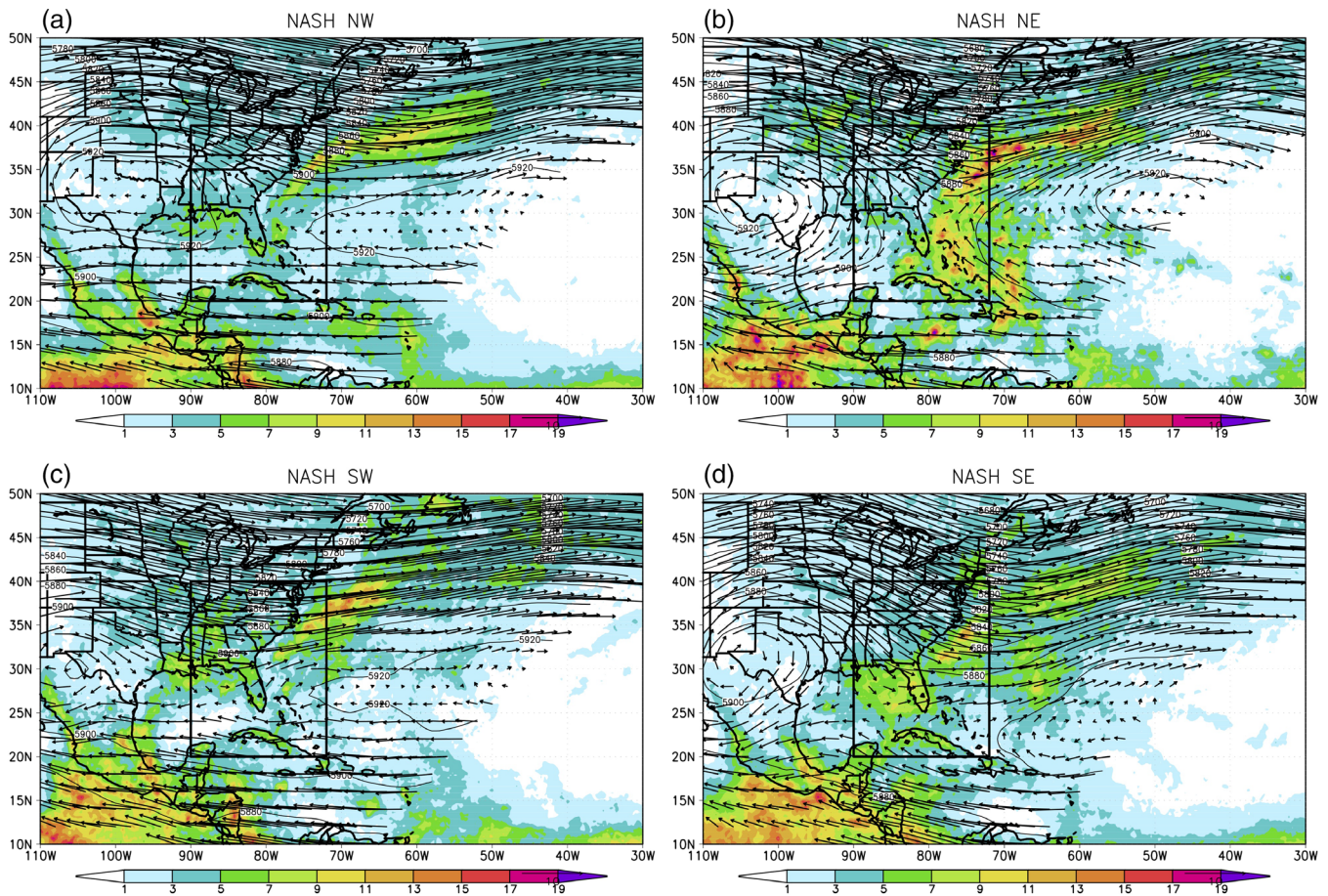
FIGURE 6 Composites of TRMM precipitation (shaded, mm·day^{-1}), and NARR 500 hPa winds (vectors, m·s^{-1}), and geopotential height (contours, m) for each NASH western ridge regime. The 1,560 m contour is thicker and boxes mark the location of the NMQ domain [Colour figure can be viewed at wileyonlinelibrary.com]

TABLE 2 Domain-averaged IPF, MPF, and total precipitation (mm·day^{-1}) for each quadrant and for all JJA 2009–2012 days combined

	NASH-NW	**NASH-NE**	**NASH-SW**	**NASH-SE**	**All-days**
IPF	1.23 (+0.01)	1.24 (+0.02)	**1.31 (+0.09)**	**1.16 (−0.06)**	1.22
MPF	**2.00 (−0.26)**	2.46 (+0.18)	2.46 (+0.19)	**2.47 (+0.20)**	2.27
Total	**3.23 (−0.27)**	3.70 (+0.20)	3.77 (+0.28)	3.63 (0.14)	3.49

Note: Anomalies for each quadrant with respect to the all-days average are shown in parentheses (mm·day^{-1}). Statistically significant values (95% in Student's *t* test) are printed in bold. All averages are for the NMQ domain shown in Figure 2.

(Figure 7c) over the southern tier of the SE US and surrounding ocean. When considered as a whole, these results suggest a connection between the lower and upper-tropospheric synoptic scale circulation and the location of the MPF precipitation anomalies across the domain.

4 | DISCUSSION

This work extends our current understanding of the influence of the summertime NASH western ridge on SE

US precipitation to the study of its influence on daily precipitation variability and organization across the region. While previous studies found that the position of the NASH western ridge controls seasonal mean precipitation in the SE US, this study showed that the NASH western ridge also plays an important role in modulating day-to-day precipitation variability in the SE US. Namely, the NASH western ridge influenced the amount, regional distribution and also the organization of precipitation across the SE US and the adjacent Atlantic Ocean.

This study showed that the location of the NASH western ridge affected regional precipitation organization into IPF and MPF. The link between low-level jets and

FIGURE 7 Composites of NMQ Total, IPF and MPF precipitation anomalies (mm·day^{-1}) greater than the 95% significance level for (a–c) NASH-NW, (d–f) NASH-SW, (g–i) NASH-NE, (j–l) NASH-SE [Colour figure can be viewed at wileyonlinelibrary.com]
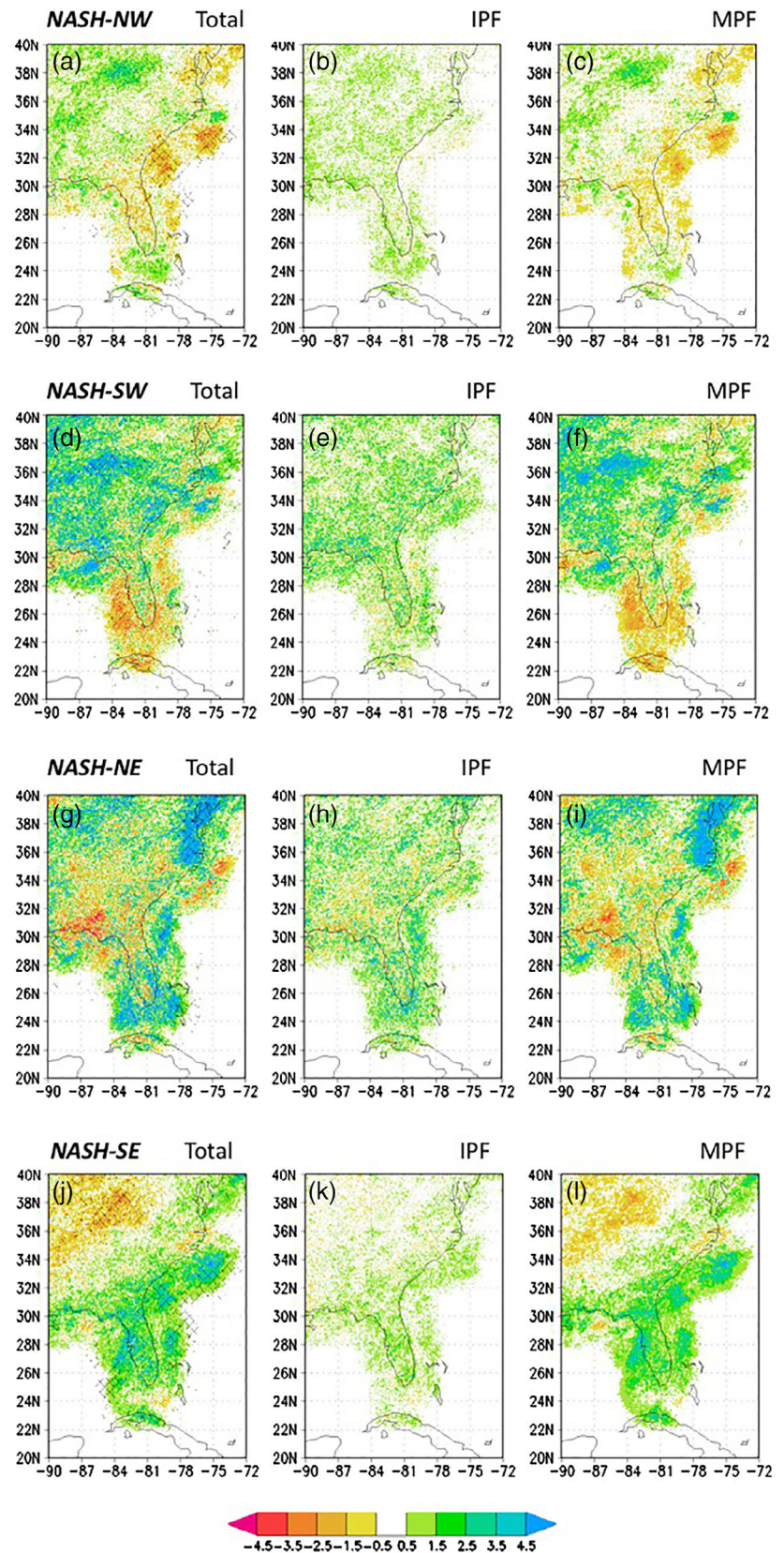
deep convection have long been recognized (Stensrud, 1996), and the GPLLJ in particular has been previously shown to play an important role in modulating precipitation in the central and eastern United States (e.g., Higgins *et al*., 1997). The NASH control on precipitation has been shown to occur via changes in the position of the low-level jets that flank the NASH western ridge and act as corridors of water vapour transport to

fuel precipitation (Higgins *et al*., 1997). In this study the position of the low-level jets on the western side of the NASH was shown to affect mainly the amount and location of larger precipitation features, that is MPF, which are known to respond to dynamic forcing (e.g., R15; Leary and Houze, 1979; Laing and Fritsch, 2000; Rickenbach *et al*., 2002). The location of the dynamical features (850 hPa winds and moisture flux, and 500 hPa trough) was shown to correspond to maxima in MPF rain as described earlier (Figures 4–7), especially in NASH-NW, NASH-SW and NASH-SE. The IPF precipitation indicated higher than average anomalies for NASH-SW (Figure 7e) and NASH-NE (Figure 7h), which are the two composites that also had the highest MPF anomalies. However, unlike the MPF anomalies, the IPF positive anomalies were distributed more uniformly across the SE US. R15 suggested that IPF rain across the SE US is modulated generally by daytime instability particularly in the coastal plain regions. Nevertheless, there were no notable differences in the values of stability indices (such as CAPE and lifted index) among the NASH composites that might explain the enhanced IPF in the SW and NE quadrants. The spatial uniformity of the IPF positive anomalies suggests a general enhancement of isolated storms across the SE US for the NASH western ridge locations (SW and NE quadrants) where precipitation generally is favoured.

The influence of transient weather systems such as midlatitude cyclones and tropical cyclones is also noteworthy. For instance, on August 22, 2009 Hurricane Bill disrupted the NASH as it recurved along the East Coast, likely contributing to the observed eastward shift of the NASH western ridge (Figure 3) from NASH-SW to NASH-SE. Additionally, although summertime midlatitude cyclones that affect the SE US are weaker and less numerous than their winter counterparts (Nieto Ferreira *et al*., 2013; Nieto Ferreira and Hall, 2015) they can also disrupt the NASH and contribute to eastward shifts in the position of the NASH western ridge. For instance, on July 12–14, 2011 a cold front associated with a midlatitude cyclone in Canada approached the SE US from the west contributing to a 45° eastward shift on the western ridge of the NASH—from NASH-NW to NASH-SE (Figure 3). The patterns of low-level winds and precipitation during a typical summertime midlatitude cyclone passage in the SE US shown in the composites in fig. 5 of Nieto Ferreira *et al*. (2013) resemble the NASH composites in Figure 4. For instance, comparison of these two sets of composites shows that the NASH-NW composite (Figure 4a) resembles days −3 and −2 (fig. 5a,b of Nieto Ferreira *et al*., 2013) of the composite of a summertime midlatitude cyclone passage in the SE US. Likewise NASH-SW resembles day −1 (fig. 5c of Nieto Ferreira

et al., 2013), NASH-NE (Figure 4b) resembles day 0 (fig. 5d of Nieto Ferreira *et al*., 2013), and NASH-SE resembles days +1 and + 2 (fig. 5e,f of Nieto Ferreira *et al*., 2013). This suggests that during a summertime midlatitude cyclone passage across the SE US the NASH western ridge shifts from NASH-NW to NASH-SW ahead of the cyclone, followed by NASH-NE on day 0 and NASH-SE after the cyclone passage.

Finally, analysis of the day-to-day variability of the NASH western ridge regional patterns of precipitation organization also revealed the presence of a summertime precipitation dipole in the SE US. Most of the summer (about 74% of all days) the NASH western ridge was located in the NW and SE quadrants, often spending five or more consecutive days at a time in each quadrant. This is significant because the NASH-NW and NASH-SE composites have generally opposite precipitation anomaly patterns, forming a dipole between the coastal/oceanic regions and the interior of the SE US. The NASH-SE periods tend to be drier inland and wetter along the coast, Florida peninsula, and offshore (Figure 7j). On the other hand, the NASH-NW periods have more rain inland and less rain along the coast, Florida, and offshore (Figure 7a). The summer dipole pattern is most pronounced in the MPF precipitation anomalies. However, it is also present in the IPF during NASH-SE, when the IPF precipitation anomalies mirror the MPF anomalies, with an inland deficit and a coastal and offshore enhancement. The dipole pattern of wetter inland/drier coastal and drier inland/wetter coastal regimes generally encapsulates the seasonal variability of summertime precipitation in the SE US, with NASH-SE more often occurring in early and late summer and NASH-NW occurring more often in midsummer (Figure 3). Over the Caribbean, the midsummer dominance of the NASH-NW can lead to higher sea level pressure and less precipitation (Figure 4a), a feature known as the Caribbean midsummer drought (Gamble *et al*., 2008).

5 | CONCLUSIONS

This study analysed 4 years of R15 precipitation organization data, TRMM precipitation and NARR Reanalysis to study the effect of the NASH western ridge on precipitation organization in the SE US. It was found that the NASH western ridge played a notable effect on precipitation organization, as summarized below.

The NASH western ridge displayed notable variability on diurnal-to-seasonal timescales. For the purposes of this study the position of the NASH western ridge was defined as the westernmost point in the 1,560 hPa contour of the 850 hPa NARR geopotential. The mean

summertime position of the NASH western ridge was determined and used to divide the study domain into four quadrants. The daily position of the NASH was then classified as NASH-NW, NASH-SW, NASH-NE, and NASH-SE. Each summer the NASH western ridge advanced westward towards the SE US from June to July and then retreated eastward thereafter. Superimposed on this seasonal propagation there was a day-to-day variability of the NASH western ridge position. The NASH western ridge was located in the NASH-NW and NASH-SE quadrants most (74%) of the time, clustering in time with occasional shorter incursions into the NASH-SW and NASH-NE quadrants. Some of this day-to-day variability in the position of the NASH western ridge may be linked to the passage of midlatitude and tropical cyclones through the study region. Quantification of the role of cyclones on the variability of the position of the western ridge of the NASH is an important subject for future study. Some of the day-to-day variability of the NASH western ridge was also recently shown (Wei *et al*., 2019) to be linked to an intraseasonal mode of variability in the 10–20 day timescale.

The effect of the NASH western ridge on precipitation organization was studied using composites of NARR reanalysis and the R15 precipitation feature dataset, which classified precipitation into IPF and MPF. In line with previous studies (R15; Nesbitt *et al*., 2006) MPF precipitation contributed most (about 65%) of the summertime precipitation in the SE US and accounted for most of the regional precipitation differences between the four NASH quadrants. IPF rain was found to be more uniformly distributed across the SE US. In general, MPF precipitation had regional variability that was tied to the presence of low-level jets (GPLLJ and the Western Atlantic LLJ), which were in turn controlled by the position of the NASH western ridge. The position of the NASH western ridge was shown to influence the synoptic scale environment that controls precipitation variability and organization in the SE US. During summer, the rainiest days—measured in terms of domain-averaged precipitation—occurred when the NASH western ridge persisted for a few days at a time in the southwest quadrant (NASH-SW). During those days, strong southwesterly winds associated with an eastward turn of the GPLLJ fuelled widespread positive MPF rain anomalies over the SE US. Slightly lower domain-averaged precipitation occurred during NASH-NE days, when the western Atlantic low-level jet was located just offshore of the southeastern coastal plain. During NASH-NE however, the region of maximum MPF rain anomaly occurred in the mid-Atlantic region, where moisture fluxes from the western Atlantic jet converged with westerly winds from the continent.

A new dipole pattern of precipitation involving NASH-NW and NASH-SE was found to be a dominant feature of the summer variability in the SE US. During most of the summer, the NASH western ridge was present in the NASH-NW (41% of the days) or NASH-SE quadrants (34% of the days) for several days to nearly a couple of weeks at a time. The driest periods in this study occurred when the NASH western ridge was on the northwest quadrant (NASH-NW), generally early or late in the summer. During NASH-NW the western ridge reached into the SE US bringing higher 850 hPa geopotential and making the GPLLJ go around most of the SE US, with the result of suppressing the formation of MPF rain along the coastal SE US, Florida, and offshore. The opposite precipitation pattern anomaly occurred during NASH-SE, generally in midsummer. NASH-SE periods tended to last for several days to a week at a time and were characterized by enhanced MPF and IPF rain over the coastal SE US, Florida and offshore, and decreased MPF and IPF rain inland. This precipitation dipole is controlled by the position of the NASH western ridge and the strength and location of its associated low-level jets. A detailed investigation of the SE US summertime precipitation organization dipole using a longer timeseries merits future study.

ORCID

Rosana Nieto Ferreira https://orcid.org/0000-0001-7341-566X

REFERENCES

Arias, P.A., Fu, R. and Mo, K.C. (2012) Decadal variation of rainfall seasonality in the North American monsoon region and its potential causes. *Journal of Climate*, 25, 4258–4274. https://doi.org/10.1175/JCLI-D-11-00140.1.

Bishop, D.A., Williams, A.P., Seager, R., Fiore, A.M., Cook, B.I., Mankin, J.S., Singh, D., Smerdon, J.E. and Rao, M.P. (2019) Investigating the causes of increased twentieth-century fall precipitation over the southeastern United States. *Journal of Climate*, 32, 575–590. https://doi.org/10.1175/JCLI-D-18-0244.1.

Bowerman, A.R., Fu, R., Yin, L., Fernando, D.N., Arias, P.A. and Dickinson, R.E. (2017) An influence of extreme Southern Hemisphere cold surges on the North Atlantic Subtropical High

through a shallow atmospheric circulation. *Journal of Geophysical Research – Atmospheres*, 122, 10135–10148. https://doi.org/10.1002/2017JD026697.

Cherchi, A., Ambrizzi, T., Behera, S., Freitas, A., Morioka, Y. and Zhou, T. (2018) The response of subtropical highs to climate change. *Current Climate Change Reports*, 4, 371–382. https://doi.org/10.1007/s40641-018-0114-1.

Colbert, A.J. and Soden, B.J. (2012) Climatological variations in North Atlantic tropical cyclone tracks. *Journal of Climate*, 25, 657–673. https://doi.org/10.1175/JCLI-D-11-00034.1.

Colle, B.A. and Novak, D.R. (2010) The New York bight jet: climatology and dynamical evolution. *Monthly Weather Review*, 138, 2385–2404. https://doi.org/10.1175/2009MWR3231.1.

Cortesi, N., Gonzalez-Hidalgo, J., Trigo, R.M. and Ramos, A.M. (2014) Weather types and spatial variability of precipitation in the Iberian Peninsula. *International Journal of Climatology*, 34, 2661–2677. https://doi.org/10.1002/joc.3866.

Davis, R.E., Hayden, B.P., Gay, D.A., Phillips, W.L. and Jones, G.V. (1997) The North Atlantic subtropical anticyclone. *Journal of Climate*, 10, 728–744.

Diem, J.E. (2006) Synoptic-scale controls of summer precipitation in the southeastern United States. *Journal of Climate*, 19, 613–621. https://doi.org/10.1175/JCLI3645.1.

Diem, J.E. (2013a) Comments on "Changes to the North Atlantic Subtropical High and its role in the intensification of summer rainfall variability in the southeastern United States". *Journal of Climate*, 26, 679–682. https://doi.org/10.1175/JCLI-D-11-00390.1.

Diem, J.E. (2013b) Influences of the Bermuda High and atmospheric moistening on changes in summer rainfall in the Atlanta, Georgia region, USA. *International Journal of Climatology*, 33, 160–172. https://doi.org/10.1002/joc.3421.

Doubler, D.L., Winkler, J.A., Bian, X., Walters, C.K. and Zhong, S. (2015) An NARR-derived climatology of southerly and northerly low-level jets over North America and coastal environs. *Journal of Applied Meteorology and Climatology*, 54, 1596–1619. https://doi.org/10.1175/JAMC-D-14-0311.1.

Gamble, D.W., Parnell, D.B. and Curtis, S. (2008) Spatial variability of the Caribbean mid-summer drought and relation to North Atlantic high circulation. *International Journal of Climatology*, 28, 343–350. https://doi.org/10.1002/joc.1600.

He, C., Wu, B., Zou, L. and Zhou, T. (2017) Responses of the summertime subtropical anticyclones to global warming. *Journal of Climate*, 30, 6465–6479. https://doi.org/10.1175/JCLI-D-16-0529.1.

Helmis, C., Wang, Q., Sgouros, G., Wang, S. and Halios, C. (2013) Investigating the summertime low-level jet over the East Coast of the U.S.A.: a case study. *Boundary-Layer Meteorology*, 149, 259–276. https://doi.org/10.1007/s10546-013-9841-y.

Higgins, R.W., Yao, Y., Yarosh, E.S., Janowiak, J.E. and Mo, K.C. (1997) Influence of the Great Plains low-level jet on summertime precipitation and moisture transport over the central United States. *Journal of Climate*, 10, 481–507.

Houze, R.A., Smull, B.F. and Dodge, P. (1990) Mesoscale organization of springtime rainstorms in Oklahoma. *Monthly Weather Review*, 118, 613–654.

Huffman, G.J., Bolvin, D.T., Nelkin, E.J., Wolff, D.B., Adler, R.F., Gu, G., Hong, Y., Bowman, K.P. and Stocker, E.F. (2007) The TRMM multisatellite precipitation analysis (TMPA): quasi-global, multiyear, combined-sensor precipitation estimates at fine scales. *Journal of Hydrometeorology*, 8, 38–55. https://doi.org/10.1175/JHM560.1.

Jones, C. (2019) Recent changes in the South America low-level jet. *npj Climate and Atmospheric Science*, 2, 20. https://doi.org/10.1038/s41612-019-0077-5.

Kalnay, E., Kanamitsu, M., Kistler, R., Collins, W., Deaven, D., Gandin, L., Iredell, M., Saha, S., White, G., Woollen, J., Zhu, Y., Chelliah, M., Ebisuzaki, W., Higgins, W., Janowiak, J., Mo, K.C., Ropelewski, C., Wang, J., Leetmaa, A., Reynolds, R., Jenne, R. and Joseph, D. (1996) The NCEP/NCAR 40-year reanalysis project. *Bulletin of the American Meteorological Society*, 77, 437–472.

Laing, A.G. and Fritsch, J.M. (2000) The large-scale environments of the global populations of mesoscale convective complexes. *Monthly Weather Review*, 128, 2756–2776.

Leary, C.A. and Houze, R.A. (1979) The structure and evolution of convection in a tropical cloud cluster. *Journal of the Atmospheric Sciences*, 36, 437–457.

Li, L., Li, W. and Deng, Y. (2013) Summer rainfall variability over the southeastern United States and its intensification in the 21st century as assessed by CMIP5 models. *Journal of Geophysical Research – Atmospheres*, 118, 340–354. https://doi.org/10.1002/jgrd.50136.

Li, L., Li, W. and Kushnir, Y. (2012) Variation of the North Atlantic Subtropical High western ridge and its implication to southeastern US summer precipitation. *Climate Dynamics*, 39, 1401–1412. https://doi.org/10.1007/s00382-011-1214-y.

Li, W., Li, L., Fu, R., Deng, Y. and Wang, H. (2011) Changes to the North Atlantic Subtropical High and its role in the intensification of summer rainfall variability in the southeastern United States. *Journal of Climate*, 24, 1499–1506. https://doi.org/10.1175/2010JCLI3829.1.

Luchetti, N.T., Nieto Ferreira, R., Rickenbach, T.M., Nissenbaum, M.R. and McAuliffe, J.D. (2017) Influence of the North Atlantic Subtropical High on wet and dry sea-breeze events in North Carolina, United States. *Investigaciones Geográficas*, 68, 9–25. https://doi.org/10.14198/INGEO2017.68.01.

Mesinger, F., DiMego, G., Kalnay, E., Mitchell, K., Shafran, P.C., Ebisuzaki, W., Jović, D., Woollen, J., Rogers, E., Berbery, E.H., Ek, M.B., Fan, Y., Grumbine, R., Higgins, W., Li, H., Lin, Y., Manikin, G., Parrish, D. and Shi, W. (2006) North American regional reanalysis. *Bulletin of the American Meteorological Society*, 87, 343–360. https://doi.org/10.1175/BAMS-87-3-343.

Muñoz, E., Busalacchi, A.J., Nigam, S. and Ruiz-Barradas, A. (2008) Winter and summer structure of the Caribbean low-level jet. *Journal of Climate*, 21, 1260–1276. https://doi.org/10.1175/2007JCLI1855.1.

Nesbitt, S.W., Cifelli, R. and Rutledge, S.A. (2006) Storm morphology and rainfall characteristics of TRMM precipitation features. *Monthly Weather Review*, 134, 2702–2721. https://doi.org/10.1175/MWR3200.1.

Nieto Ferreira, R. and Hall, L.E. (2015) Midlatitude cyclones in the southeastern United States: frequency and structure differences by cyclogenesis region. *International Journal of Climatology*, 35, 3798–3811. https://doi.org/10.1002/joc.4247.

Nieto Ferreira, R., Hall, L. and Rickenbach, T.M. (2013) A climatology of the structure, evolution, and propagation of midlatitude cyclones in the Southeast United States. *Journal of Climate*, 26, 8406–8421. https://doi.org/10.1175/JCLI-D-12-00657.1.

Parker, M.D. and Ahijevych, D.A. (2007) Convective episodes in the east-central United States. *Monthly Weather Review*, 135, 3707–3727. https://doi.org/10.1175/2007MWR2098.1.

Parker, M.D. and Johnson, R.H. (2000) Organizational modes of midlatitude mesoscale convective systems. *Monthly Weather Review*, 128, 3413–3436.

Rickenbach, T. (2018) Seasonal changes of extremes in isolated and mesoscale precipitation for the southeastern United States. *Atmosphere*, 9, 309. https://doi.org/10.3390/atmos9080309.

Rickenbach, T., Nieto Ferreira, R. and Wells, H. (2020) Springtime onset of isolated convection precipitation across the southeastern United States: Framework and regional evolution. *Monthly Weather Review*, 148(3), 891–906. https://doi.org/10.1175/MWR-D-19-0279.1.

Rickenbach, T.M., Nieto Ferreira, R., Halverson, J.B., Herdies, D.L., Dias, S. and Maria, A.F. (2002) Modulation of convection in the southwestern Amazon basin by extratropical stationary fronts. *Journal of Geophysical Research*, 107, LBA 7–LBA 13. https://doi.org/10.1029/2000JD000263.

Rickenbach, T.M., Nieto Ferreira, R., Zarzar, C. and Nelson, B. (2015) A seasonal and diurnal climatology of precipitation organization in the southeastern United States. *Quarterly Journal of the Royal Meteorological Society*, 141, 1938–1956. https://doi.org/10.1002/qj.2500.

Schmidt, D.F. and Grise, K.M. (2019) Impacts of subtropical highs on summertime precipitation in North America. *Journal of Geophysical Research – Atmospheres*, 124, 11188–11204. https://doi.org/10.1029/2019JD031282.

Stensrud, D.J. (1996) Importance of low-level jets to climate: a review. *Journal of Climate*, 9, 1698–1711. https://doi.org/10.1175/1520-0442(1996)0092.0.CO;2.

Wallace, J.M. (1975) Diurnal variations in precipitation and thunderstorm frequency over the conterminous United States. *Monthly Weather Review*, 103, 406–419.

Wang, Y., Jia, B., Wang, S., Estes, M., Shen, L. and Xie, Y. (2016) Influence of the Bermuda High on interannual variability of summertime ozone in the Houston–Galveston–Brazoria region. *Atmospheric Chemistry and Physics*, 16, 15265–15276. https://doi.org/10.5194/acp-16-15265-2016.

Wei, W., Li, W., Deng, Y. and Yang, S. (2019) Intraseasonal variation of the summer rainfall over the southeastern United States. *Climate Dynamics*, 53, 1171–1183. https://doi.org/10.1007/s00382-018-4345-6.

Zhang, D., Zhang, S. and Weaver, S.J. (2006) Low-level jets over the mid-Atlantic states: warm-season climatology and a case study. *Journal of Applied Meteorology and Climatology*, 45, 194–209. https://doi.org/10.1175/JAM2313.1.

Zhang, J., Howard, K., Langston, C., Vasiloff, S., Kaney, B., Arthur, A., Van Cooten, S., Kelleher, K., Kitzmiller, D., Ding, F., Seo, D., Wells, E. and Dempsey, C. (2011) National mosaic and multi-sensor QPE (NMQ) system: description, results, and future plans. *Bulletin of the American Meteorological Society*, 92, 1321–1338. https://doi.org/10.1175/2011BAMS-D-11-00047.1.